

**8.5%**

Date: 2021-11-01 19:23 UTC

\* All sources 42 | Internet sources 27 | Plagiarism Prevention Pool 15

- ✓ [0] [www.researchgate.net/publication/311088172\\_A\\_new\\_approach\\_for\\_the\\_interpretation\\_of\\_magnetic\\_data\\_by\\_a\\_2-D\\_dipping\\_dike](https://www.researchgate.net/publication/311088172_A_new_approach_for_the_interpretation_of_magnetic_data_by_a_2-D_dipping_dike)  
2.6% 20 matches
- ✓ [1] [www.researchgate.net/publication/331686048\\_Aeromagnetic\\_data\\_interpretation\\_for\\_delineation\\_of\\_the\\_subsurface\\_structures\\_of\\_the\\_area\\_east\\_Qena\\_pr](https://www.researchgate.net/publication/331686048_Aeromagnetic_data_interpretation_for_delineation_of_the_subsurface_structures_of_the_area_east_Qena_pr)  
1.8% 15 matches
- ✓ [2] [from a PlagScan document dated 2018-09-04 12:31](#)  
1.3% 15 matches
- ✓ [3] [from a PlagScan document dated 2018-04-11 14:53](#)  
1.5% 10 matches
- ✓ [4] [www.researchgate.net/publication/271953112\\_A\\_New\\_Method\\_for\\_Depth\\_and\\_Shape\\_Determinations\\_from\\_Magnetic\\_Data](https://www.researchgate.net/publication/271953112_A_New_Method_for_Depth_and_Shape_Determinations_from_Magnetic_Data)  
1.8% 8 matches
- ✓ [5] [www.researchgate.net/publication/276776509\\_Depth\\_and\\_shape\\_solutions\\_from\\_second\\_moving\\_average\\_residual\\_magnetic\\_anomalies](https://www.researchgate.net/publication/276776509_Depth_and_shape_solutions_from_second_moving_average_residual_magnetic_anomalies)  
1.1% 10 matches
- ✓ [6] [www.researchgate.net/publication/340438718\\_IJSRSET1621120\\_Geophysical\\_and\\_Chemical\\_Analysis\\_of\\_Iron\\_ORE\\_Deposits\\_in\\_Maua\\_Kenya](https://www.researchgate.net/publication/340438718_IJSRSET1621120_Geophysical_and_Chemical_Analysis_of_Iron_ORE_Deposits_in_Maua_Kenya)  
1.3% 7 matches
- ✓ [7] [www.mdpi.com/2076-3263/8/1/4/htm](https://www.mdpi.com/2076-3263/8/1/4/htm)  
0.5% 10 matches
- ✓ [8] [www.researchgate.net/publication/228558473\\_Generalized\\_feature\\_extraction\\_for\\_structural\\_pattern\\_recognition\\_in\\_time-series\\_data](https://www.researchgate.net/publication/228558473_Generalized_feature_extraction_for_structural_pattern_recognition_in_time-series_data)  
0.4% 7 matches
- ✓ [9] [www.researchgate.net/publication/295085890\\_Tectonic\\_units\\_and\\_proto-basin\\_of\\_the\\_East\\_China\\_Sea\\_Shelf\\_Basin\\_Correlation\\_to\\_Mesozoic\\_subduction](https://www.researchgate.net/publication/295085890_Tectonic_units_and_proto-basin_of_the_East_China_Sea_Shelf_Basin_Correlation_to_Mesozoic_subduction)  
0.0% 8 matches
- ✓ [10] [www.researchgate.net/figure/Regional-map-of-the-Egyptian-Eastern-Desert-and-Sinai-basement-rocks-showing-the-North\\_fig1\\_257588829](https://www.researchgate.net/figure/Regional-map-of-the-Egyptian-Eastern-Desert-and-Sinai-basement-rocks-showing-the-North_fig1_257588829)  
0.6% 4 matches
- ✓ [11] [www.semanticscholar.org/paper/The-significance-of-gneissic-rocks-and-synmagmatic-Fowler-Ali/a68f32907741cdd33c4a7aa958ee299118c8ff1d](https://www.semanticscholar.org/paper/The-significance-of-gneissic-rocks-and-synmagmatic-Fowler-Ali/a68f32907741cdd33c4a7aa958ee299118c8ff1d)  
0.5% 5 matches
- ✓ [12] [www.mdpi.com/1424-8220/17/8/1878/htm](https://www.mdpi.com/1424-8220/17/8/1878/htm)  
0.2% 6 matches  
1 documents with identical matches
- ✓ [14] [www.researchgate.net/publication/228579258\\_Three-dimensional\\_seismic\\_analysis\\_of\\_high-amplitude\\_anomalies\\_in\\_the\\_shallow\\_subsurface\\_of\\_the\\_Nor](https://www.researchgate.net/publication/228579258_Three-dimensional_seismic_analysis_of_high-amplitude_anomalies_in_the_shallow_subsurface_of_the_Nor)  
0.2% 5 matches
- ✓ [15] [www.researchgate.net/publication/312326228\\_Comparision\\_of\\_Edge\\_Detection\\_Methods\\_for\\_Obstacles\\_Detection\\_in\\_a\\_Mobile\\_Robot\\_Environment](https://www.researchgate.net/publication/312326228_Comparision_of_Edge_Detection_Methods_for_Obstacles_Detection_in_a_Mobile_Robot_Environment)  
0.5% 3 matches
- ✓ [16] [from a PlagScan document dated 2021-02-19 10:41](#)  
0.4% 4 matches
- ✓ [17] [www.researchgate.net/figure/Areal-map-of-the-studied-region\\_fig1\\_235424708](https://www.researchgate.net/figure/Areal-map-of-the-studied-region_fig1_235424708)  
0.2% 4 matches
- ✓ [18] [www.researchgate.net/publication/252893744\\_Control\\_circuit\\_design\\_of\\_novel\\_partial\\_gating\\_detector\\_by\\_liquid\\_crystal](https://www.researchgate.net/publication/252893744_Control_circuit_design_of_novel_partial_gating_detector_by_liquid_crystal)  
0.3% 4 matches
- ✓ [19] [pubs.usgs.gov/of/1986/0268/report.pdf](https://pubs.usgs.gov/of/1986/0268/report.pdf)  
0.0% 4 matches
- ✓ [20] [from a PlagScan document dated 2019-09-30 08:56](#)  
0.4% 2 matches
- ✓ [21] [www.researchgate.net/figure/Euler-depth-solutions-along-magnetic-anomaly-profile-BB-The-Euler-solutions-along-the\\_fig2\\_266233822](https://www.researchgate.net/figure/Euler-depth-solutions-along-magnetic-anomaly-profile-BB-The-Euler-solutions-along-the_fig2_266233822)  
0.2% 3 matches
- ✓ [22] [from a PlagScan document dated 2019-03-01 08:46](#)  
0.3% 2 matches  
1 documents with identical matches
- ✓ [24] [link.springer.com/article/10.1140/epjc/s10052-018-6096-2](https://link.springer.com/article/10.1140/epjc/s10052-018-6096-2)  
0.0% 4 matches
- ✓ [25] [from a PlagScan document dated 2018-09-18 08:19](#)  
0.0% 2 matches
- ✓ [26] [www.researchgate.net/publication/354088867\\_Self-Supervised\\_Delineation\\_of\\_Geological\\_Structures\\_using\\_Orthogonal\\_Latent\\_Space\\_Projection](https://www.researchgate.net/publication/354088867_Self-Supervised_Delineation_of_Geological_Structures_using_Orthogonal_Latent_Space_Projection)  
0.0% 3 matches

<input checked="" type="checkbox"/> [27]	 from a PlagScan document dated 2018-05-28 18:27 <b>0.0%</b> 3 matches
<input checked="" type="checkbox"/> [28]	 from a PlagScan document dated 2020-01-22 07:18 <b>0.3%</b> 1 matches
<input checked="" type="checkbox"/> [29]	 from a PlagScan document dated 2020-06-26 08:41 <b>0.2%</b> 1 matches
<input checked="" type="checkbox"/> [30]	 from a PlagScan document dated 2017-12-10 21:56 <b>0.2%</b> 1 matches
<input checked="" type="checkbox"/> [31]	 <a href="http://www.sciencedirect.com/science/article/abs/pii/S0377839821000918">www.sciencedirect.com/science/article/abs/pii/S0377839821000918</a> <b>0.3%</b> 1 matches
<input checked="" type="checkbox"/> [32]	 <a href="http://www.researchgate.net/publication/32970953_Post-Eocene_basins_of_the_Argentine_central_Andes">www.researchgate.net/publication/32970953_Post-Eocene_basins_of_the_Argentine_central_Andes</a> <b>0.2%</b> 1 matches
<input checked="" type="checkbox"/> [33]	 from a PlagScan document dated 2021-03-29 08:18 <b>0.0%</b> 1 matches
<input checked="" type="checkbox"/> [34]	 from a PlagScan document dated 2021-01-26 11:14 <b>0.0%</b> 1 matches
<input checked="" type="checkbox"/> [35]	 from a PlagScan document dated 2021-01-04 07:20 <b>0.0%</b> 1 matches
<input checked="" type="checkbox"/> [36]	 from a PlagScan document dated 2019-01-12 04:06 <b>0.0%</b> 1 matches
<input checked="" type="checkbox"/> [37]	 <a href="http://www.researchgate.net/publication/270102618_Establishing_chronologies_for_woodland_hollow_and_mor_humus_deposits_using_tephrochronology_and_">www.researchgate.net/publication/270102618_Establishing_chronologies_for_woodland_hollow_and_mor_humus_deposits_using_tephrochronology_and_</a> <b>0.0%</b> 1 matches
<input checked="" type="checkbox"/> [38]	 <a href="http://www.researchgate.net/figure/Superposition-of-lineaments-obtained-from-a-OLI-and-b-ASTER-images-in-addition-to_fig4_319920570">www.researchgate.net/figure/Superposition-of-lineaments-obtained-from-a-OLI-and-b-ASTER-images-in-addition-to_fig4_319920570</a> <b>0.0%</b> 1 matches
<input checked="" type="checkbox"/> [39]	 <a href="http://www.researchgate.net/figure/Blue-band-comparison-the-image-a-shows-the-best-available-measurement-from-2009-2011_fig3_323283165">www.researchgate.net/figure/Blue-band-comparison-the-image-a-shows-the-best-available-measurement-from-2009-2011_fig3_323283165</a> <b>0.0%</b> 1 matches
<input checked="" type="checkbox"/> [40]	 <a "lineaments="" are="" href="http://books.google.co.in/books?id=a13wAAAAMAAJ&amp;pg=SL4-PA39&amp;lpg=SL4-PA39&amp;dq=" superimposed""&amp;source='bl&amp;ots=tjLTOAbBT&amp;sig="'>books.google.co.in/books?id=a13wAAAAMAAJ&amp;pg=SL4-PA39&amp;lpg=SL4-PA39&amp;dq=""lineaments are superimposed""&amp;source=bl&amp;ots=tjLTOAbBT&amp;sig=.</a> <b>0.0%</b> 1 matches
<input checked="" type="checkbox"/> [41]	 from a PlagScan document dated 2018-10-03 06:13 <b>0.0%</b> 1 matches
<input checked="" type="checkbox"/> [42]	 <a href="http://citeseerx.ist.psu.edu/viewdoc/download?doi=10.1.1.908.9148&amp;rep=rep1&amp;type=pdf">citeseerx.ist.psu.edu/viewdoc/download?doi=10.1.1.908.9148&amp;rep=rep1&amp;type=pdf</a> <b>0.0%</b> 1 matches
<input checked="" type="checkbox"/> [43]	 <a href="http://www.researchgate.net/publication/236157912_Pre-existing_basement_structure_and_its_influence_on_continental_rifting_and_fracture_zone_development">www.researchgate.net/publication/236157912_Pre-existing_basement_structure_and_its_influence_on_continental_rifting_and_fracture_zone_development</a> <b>0.0%</b> 1 matches

14 pages, 2290 words

**PlagLevel: 8.5% selected / 12.3% overall**

58 matches from 44 sources, of which 28 are online sources.

#### Settings

Data policy: *Compare with web sources, Check against the Plagiarism Prevention Pool*

Sensitivity: *High*

Bibliography: *Bibliography excluded*

Citation detection: *Highlighting only*

Whitelist: --

## Mapping geological structures using aeromagnetic data

### Abstract

One major purpose of interpretation of magnetic data is to highlight borders of geology structures. In this paper, we applied the edge detectors such as the enhancement of total gradient (ETG), normalized horizontal gradient (NHG), theta map (TM) and fast sigmoid (FSED) methods to delineate geological structures that appear as lineaments in transformed magnetic anomaly maps. Initially, these methods were estimated on a magnetic model for understanding their capability. Further, we applied these methods to real aeromagnetic data for determining lineaments of the Wadi Umm Dulfah area. Additionally, the magnetic sources depths in the area were also computed by the tilt depth method.<sup>[1]</sup> Findings bring a better understanding of the edge detectors capability, as well as the geology structures of the Wadi Umm Dulfah area.

Keywords: magnetics, edge detector, lineaments, geological structure.

### <sup>[0]</sup> 1. Introduction

Detection of the border and depth of anomalous bodies is one of the most important aims in magnetic and gravity interpretations (Dung and Thanh, 2016; Dung and Minh, 2017; Hang et al, 2019; Eldosouky and Saada, 2020; Pham et al., 2019; 2021a,b; Eldosouky et al., 2021a; Hoang et al., 2021; Duong et al., 2021; Eldosouky and Mohamed, 2021). The information of the borders is important in estimating the boundaries of geology formations (Pham et al., 2018a; Eldosouky et al., 2021b). There are a great number of edge detection methods developed for interpreting the potential field data (Eldosouky et al., 2020a,b; Pham 2020; Pham et al., 2021c,d). The total gradient method (TG) is one of the conventional methods that are commonly used for outlining the edges (Roest et al., 1992). Although this detector is a very popular method used to interpret magnetic data, it also has some limitations. Hsu et al. (1996) suggested using an enhancement of the TG method (ETG) to increase the resolution of the result. These detectors use the maximum location to extract the source borders. Miller and Singh (1994) proposed the tilt derivative detector to balance the different anomalies. This detector detects the borders of the geological structures by the zero contours. Wijns et al. (2005) proposed the theta map detector that normalizes the TG by the amplitude of the horizontal gradient. The negative contours of the theta map are located over

the borders of magnetic structures.<sup>[0]</sup> Cooper and Cowan (2006) proposed the normalized version of the horizontal gradient that normalizes the vertical derivative amplitude by the gradient amplitude. The method uses the maximum location to detect the borders of the geology structures. Pham et al. (2018b, 2020a) developed some detectors based on hyperbolic tangent and logistic functions that provide the maximum values over the borders of the sources. These methods bring the borders with higher resolution compared to the conventional methods.<sup>[0]</sup> Melouah and Pham (2021) proposed an improved version of logistic detector that is based on the third order derivatives of the data. Oksum et al. (2021) presented a new detector that uses the fast-sigmoid function of the gradients of the gradient amplitude. Similar to the logistic filters, this method provides an image with high resolution for the source borders, and it uses the maximum values to outline the borders.<sup>[0]</sup> In addition to the above-mentioned filters, there are many other detectors based on the derivatives of magnetic and gravity data in the literature (Cordell and Grauch; 1985; Beiki, 2010; Ferreira et al. 2013; Pham et al., 2020b, 2021e; Pham 2021).<sup>[10]</sup>

The Wadi Umm Dulfah area lies in the Egyptian North Eastern Desert (ENED) to the west of Hurghada city. The area is covered by sediments in its central and eastern parts and with basement in the western part.

In this paper, the detectors such as the enhanced total gradient (ETG), normalized horizontal gradient (NHG), theta map (TM) and fast sigmoid (FSED) have been applied to aeromagnetic data to extract geology features of the Wadi Umm Dulfah area. The effectiveness of these methods has been estimated on a magnetic model before applying to real data.

## 2. Geological setting

The Egyptian Eastern Desert (EED) is divided into three main territories. These main parts are South (ESED), Central (ECED), and North (ENED). These three domains were generated in different tectonic frameworks in an independent, but in a very similar style and exhibit a specific younging from (ESED) to (ENED). Geologically, these three domains differ from each other to their foremost revealed rock types (Kroner et al., 1987). The ENED, to the north of 27° 00' lat., is distinguished by the presence of younger rocks (e.g.,<sup>[6]</sup> Dokhan volcanics, younger Gattarian

granites, and Hammamat sediments), while the older **types of the rocks** rarely occur like the granodiorites, 610 – 680 Ma (Stern and Hedge 1985).

<sup>[10]</sup>▶ The Wadi (W) Umm Dulfah **area is located in the Egyptian** North-Eastern Desert (ENED). The main wadis cutting the area are W Faliq, W Umm Dulfah, W Umm Dhaysi, and W Umm Kharazah (EGSMA, 2005). <sup>[11]</sup>▶ The area reaches the coast of the red sea from its north-eastern side and **is covered by various rock units of different ages** (Precambrian to Recent) (Fig. 1). The basements of the ENED are a part of the Arabian Nubian Shield (ANS) which were created throughout the Pan-African era (900 to 600 Ma) in a marine setting (Kroner, 1985; Shackleton, 1994). The eastern and central parts of W Umm Dulfah area are covered by the recent Holocene deposits (Wadi deposits, Coral Reefs, Sabkha, and Alluvial wadi deposits, Pleistocene deposits, Gabir formation (F) of Pliocene age, and Samh F and Gharamul F (Miocene) (Conoco, 1987; EGSMA, 2005). The basements (western part of W Umm Dulfah area) acidic-to-intermediate metavolcanics, Gabbro-Diorite, Granodiorite-Tonalite, Monzogranite, and Alkali feldspar granite (El Gaby et al., 1990; EGSMA, 2005).

### 3. Data

The studied area was operated by Aero-Service-Aircraft, Cessna-Titan, type 404. The separation of traverse lines was 1 km and 10 km, and tie-line separation was at 120 m altitude (terrain clearance). The traverse lines were situated in a north-east:south-west (NE-SW) direction and perpendicular tie lines to the traverse direction, north-west:south-east (NW-SE) (Aero-Service-Report, 1984). <sup>[1]</sup>▶ The data is obtained in the form of **total magnetic intensity (TMI)**. The TMI data is digitized and gridded after subtracting the IGRF. <sup>[1]</sup>▶ Then, the TMI is **reduced to the north magnetic pole (RTP)**. The parameters employed for the reduction are an inclination of 39.5°N and declination of 2°E which express the mean value for the area. The RTP data range from 395 nT to 690 nT with high amplitude anomalies that appear in the southeastern regional of the Wadi Umm Dulfah area (Fig. 2).

### 4. Methods

The ETG method is one of the high-resolution methods for enhancing the borders of the geology structures. The ETG of the field F is defined by the following equation (Hsu et al., 1996):

$$ETG = \sqrt{\left(\frac{\partial^2 F}{\partial z \partial x}\right)^2 + \left(\frac{\partial^2 F}{\partial z \partial y}\right)^2 + \left(\frac{\partial^2 F}{\partial z \partial z}\right)^2} \quad (1)$$

The TM method is defined by Wijns et al. (2005). It uses the ratio of the derivatives to balance the different anomalies. Its equation is given as:

$$TM = \text{acos} \frac{\sqrt{\left(\frac{\partial F}{\partial x}\right)^2 + \left(\frac{\partial F}{\partial y}\right)^2}}{\sqrt{\left(\frac{\partial F}{\partial x}\right)^2 + \left(\frac{\partial F}{\partial y}\right)^2 + \left(\frac{\partial F}{\partial z}\right)^2}} \quad (2)$$

The NHG is another balanced method, proposed by Cooper and Cowan (2006).<sup>[5]▶</sup> The equation of the NHG is given as the following equation:

$$NHG = \text{atan} \frac{\sqrt{\left(\frac{\partial F}{\partial x}\right)^2 + \left(\frac{\partial F}{\partial y}\right)^2}}{\left|\frac{\partial F}{\partial z}\right|}. \quad (3)$$

Another detector for enhancement of the borders is introduced by Oksum et al. (2021),<sup>[0]▶</sup> which is based on the gradients of the gradient amplitude.<sup>[18]▶</sup> The detector can enhance the borders of the shallow and deep bodies at the same time. Its equation is given by:

$$\text{FSED} = \frac{R - 1}{1 + |R|} \quad (4)$$

where

$$R = \frac{\frac{\partial \text{THG}}{\partial z}}{\sqrt{\left(\frac{\partial \text{THG}}{\partial x}\right)^2 + \left(\frac{\partial \text{THG}}{\partial y}\right)^2}} \quad (5)$$

## [ 0 ] ▶ 5. Test study

Initially, we generated a synthetic magnetic model to study the effectiveness of the detectors, and its enhanced versions. The three-dimensional view of the model is displayed in Fig 3a. This model consists of three prismatic sources, whose parameters are given by Table 1. The computed magnetic anomaly over the model is displayed in Fig. 3b. Fig. 4a shows the ETG of data in Fig. 3b. We can see that, the ETG method can bring clear images for the edges for the body A, but responses from the bodies B and C are blurred. Fig. 4b shows the  $TM$  of magnetic data in Fig. 3b. Although the TM can equalize the signals from shallow and deep sources, it brings the false boundaries around the body B. Fig. 4c shows the result of application of the NHG method to magnetic data in Fig. 3b. As can be seen from this figure, the NHG is more effective in determining all the borders than ETG method. Similar to the TM method, the ETG method uses the ratio of the gradients, thus it can equalize the signals from shallow and deep bodies. However, the NHG method also brings the false boundaries around the body B. Fig. 4d displays the boundaries obtained from applying the FSED method to magnetic data in Fig. 3b. It is clearly seen that the peaks of the FSED are located directly over the source boundaries, and this detector provides sharper responses over the source boundaries than ETG, TM and NHG methods.

## 6. Results and discussion

We used the RTP map (Fig. 2) to extract the structural features of the Wadi Umm Dulfah area. Fig. 5a shows the boundaries determined by applying the ETG filter to the RTP data. We can see that the ETG filter is dominated by the anomalies with larger amplitudes in the southeastern regional, and it cannot outline the borders of the small anomalies clearly. Fig. 5b shows the result obtained by applying the  $TM$  method to the RTP data. It is clearly seen that the TM method is very effective in balancing magnetic anomalies with different amplitudes, and it provides clearer geological features compared to the ETG. Fig. 5c shows the result obtained by applying the NHG method to the RTP data. Similar to the TM method, the NHG method is also effective in bringing a balanced image of the edges, and it provides clearer lineaments compared to the ETG. Fig. 5b and 5c show that both the TM and NHG methods gave the same result. Although the TM and NHG methods are not dominated by the anomalies with larger amplitudes in the southeastern part of the area, the boundaries determined by these methods are connected,

making it hard for extracting structural features of the Wadi Umm Dulfah area. The reason is that the TM and NHG methods are based on the zero values of the vertical gradient that produces the false zero contours around the sources (Pham et al., 2021). Fig. 5d shows the result obtained from applying the FSED method to the RTP data. Clearly, the FSED detector cannot only delineate the borders of strong and weak amplitude signals at the same time, but also brings sharp responses over geological features of the Wadi Umm Dulfah area.

To estimate the depths to magnetic sources in the Wadi Umm Dulfah area, the tilt depth method (Salem et al., 2007) was used.<sup>[20]</sup> The best advantage of this method is that it does not need to use magnetization, window size or structure index. Fig. 6 shows the depths of magnetic structures in the area.<sup>[6]</sup> The obtained result shows that most of the depth of magnetic structures ranges from 0.2 to 1.4 km. Here, we used the FSED map to extract the lineaments of geological features of the Wadi Umm Dulfah area. These lineaments are superimposed on the depth map (Fig. 7). As can be seen from Fig. 7,<sup>[1]</sup> the main structures of the study area are NW–SE and NE–SW trending structures.<sup>[1]</sup> In addition, most of the lineaments determined from the FSED method are verified by the magnetic sources in Fig. 6.

The lineaments of the FSED method (Fig. 7) show that Wadi Umm Dulfah area was affected by the Gulf of Suez rifting (GOSR) system. This can be notified by the excess of the NW trends related to the GOSR system in the central and western parts bounding the basement blocks. The E–W (Tethyan or Mediterranean) trend is absent in the obtained lineaments map (Fig. 7).

NW (Gulf of Suez) and NE are the main trends affecting the area. On this Closed alternative elongated anomalies (negative and positive) have a NW trend. We can presume that the NW (younger) trend is dominant in Wadi Umm Dulfah area (Meshref et al., 1980)<sup>[1]</sup> and the area is affected by the GOSR system during Miocene.<sup>[1]</sup> The NW faults of the study area are aligned with main basement lineaments that may have developed preexisting basement structures during the rifting (Moustafa and El Shaarawy 1987; Saada, 2016).

## 7. Conclusions

The aeromagnetic data interpretation allowed us to highlight the geological features of the Wadi Umm Dulfah area.<sup>[3]</sup> This study is based on the use of the enhanced total gradient (ETG),

normalized horizontal gradient (NHG), theta map (TM), fast sigmoid (FSED) and tilt depth methods. Findings <sup>[3]</sup> show that the FSED method has permit to clearly identify the lineaments of geological features, while the tilt depth method can provide the information on the depth of structures in the Wadi Umm Dulfah area, which ranges 0.2 to 1.4 km. These results are a very useful document in better understanding of the capability of the edge detecting methods, as well as the geological structures of the Wadi Umm Dulfah area.

Figures and captions

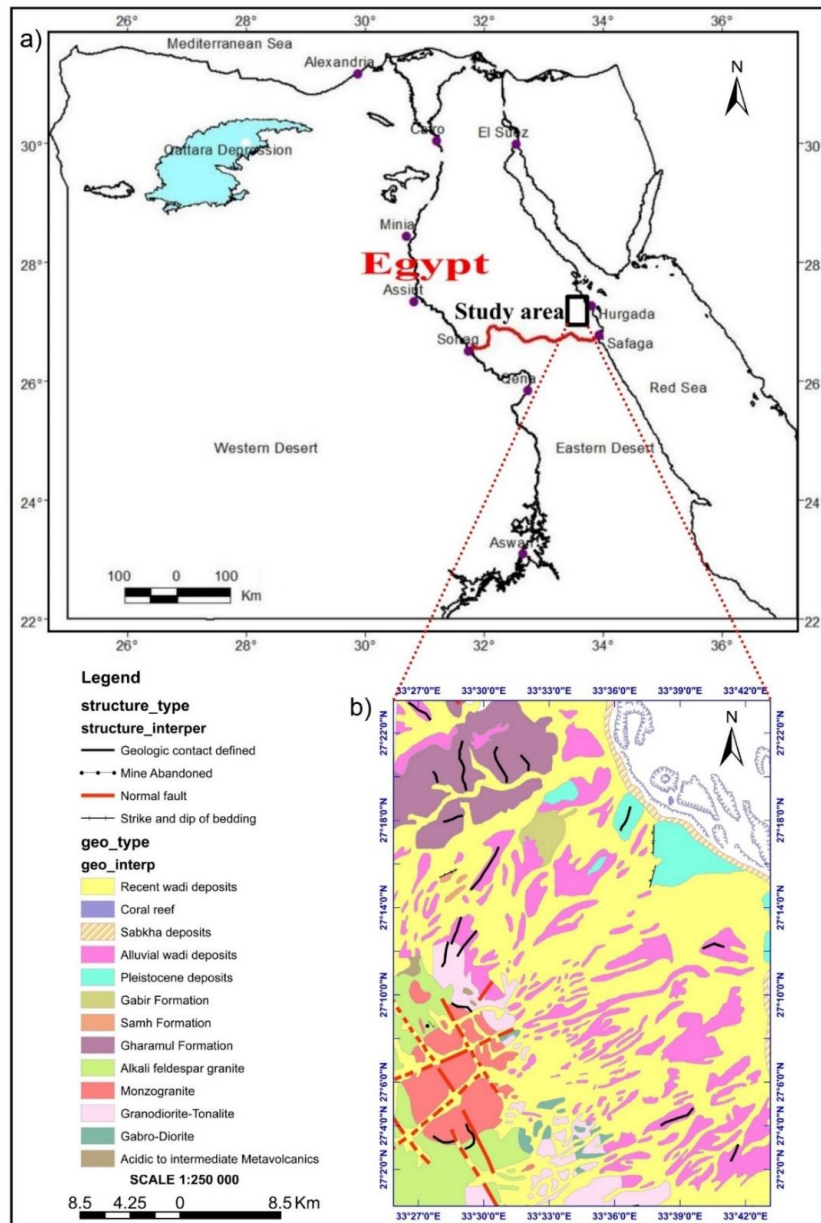


Fig. 1. a) Geographical location, b) The geology of the Wadi Umm Dulfah area (modified after EG SMA, 2005).

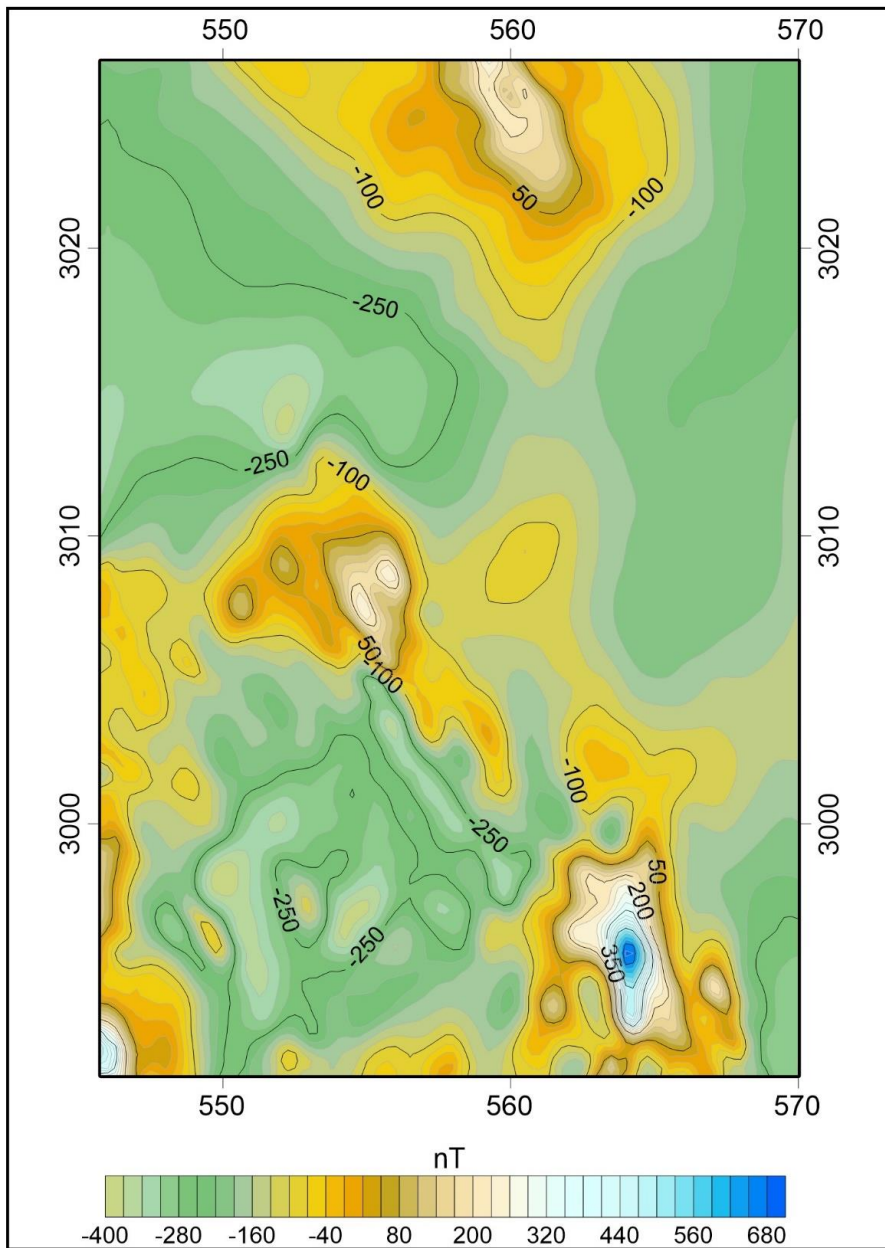


Fig. 2. RTP aeromagnetic data of the Wadi Umm Dulfah area

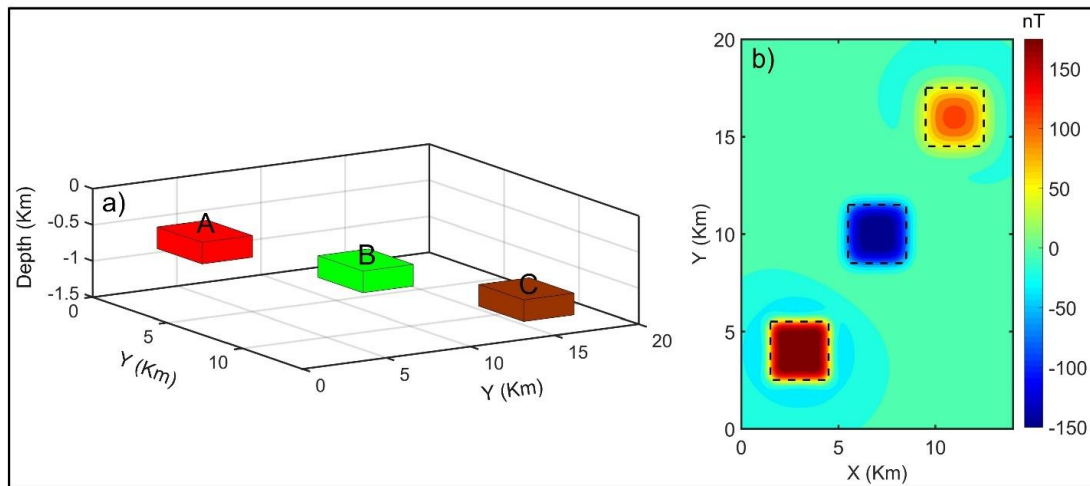


Fig. 3. Three-dimensional view of the model (a) and its magnetic anomaly (b).

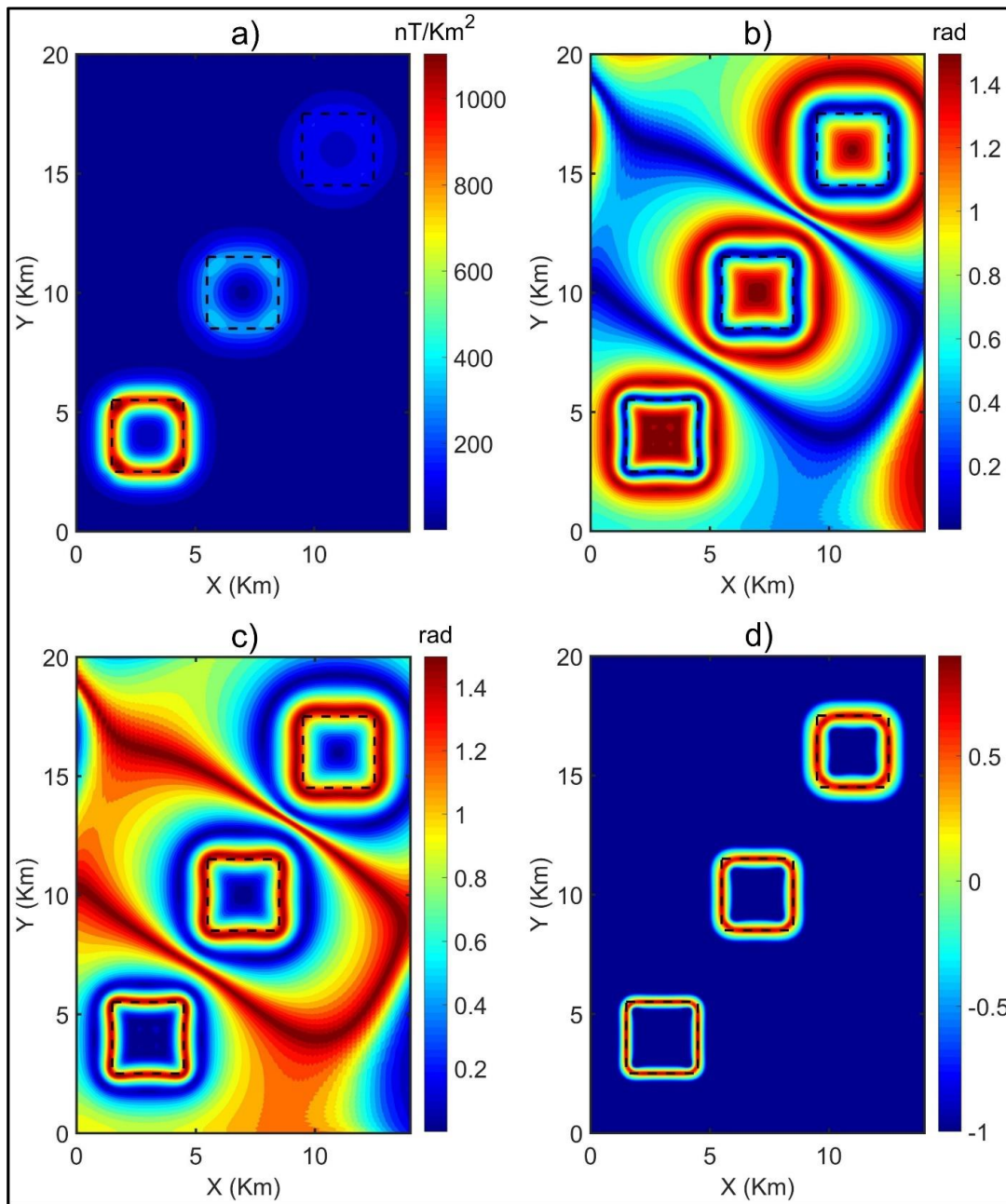


Fig. 4. a) ETG, b) TM, c) NHG, d) FSED

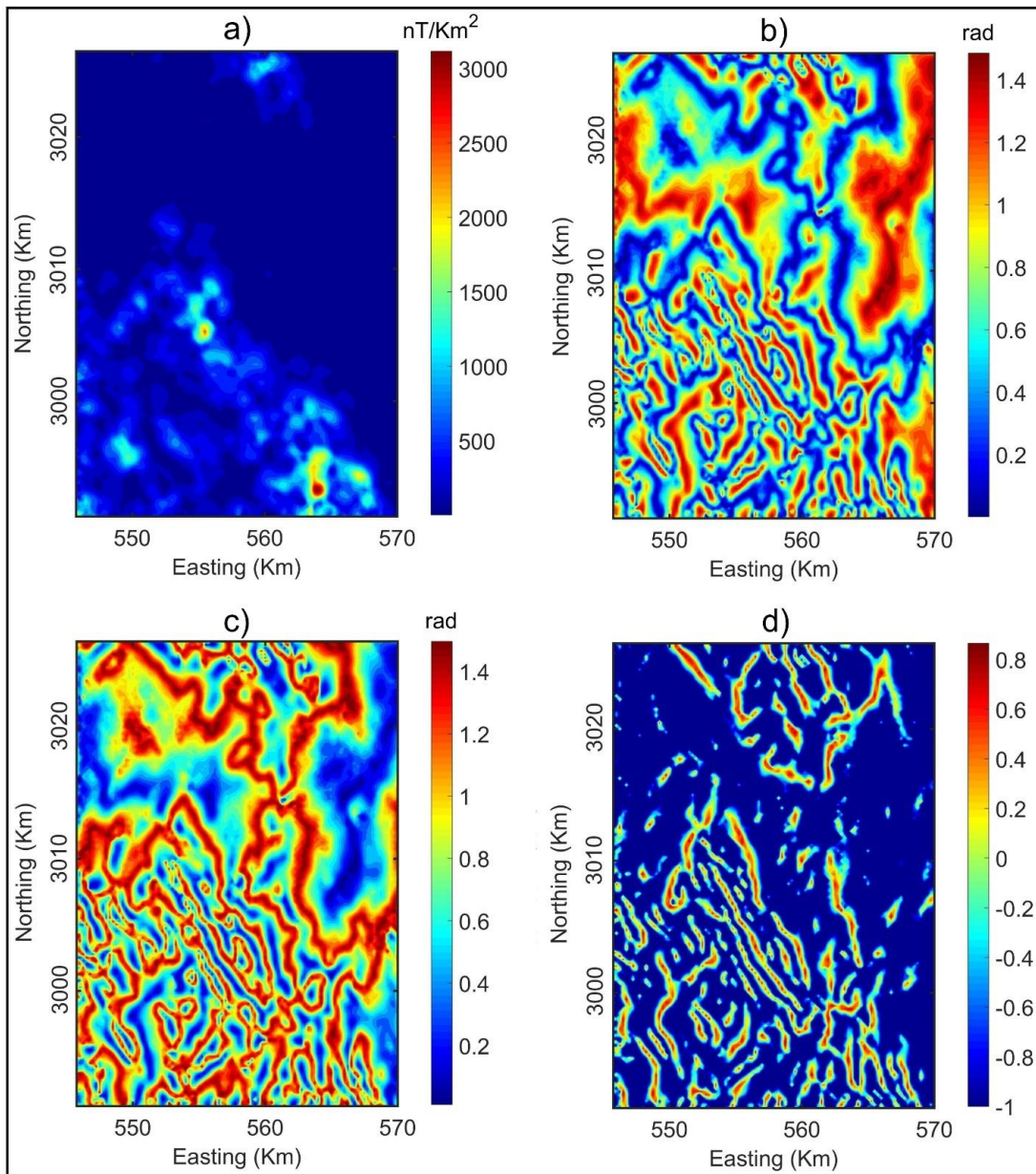


Fig. 5. a) ETG, b) TM, c) NHG, d) FSED

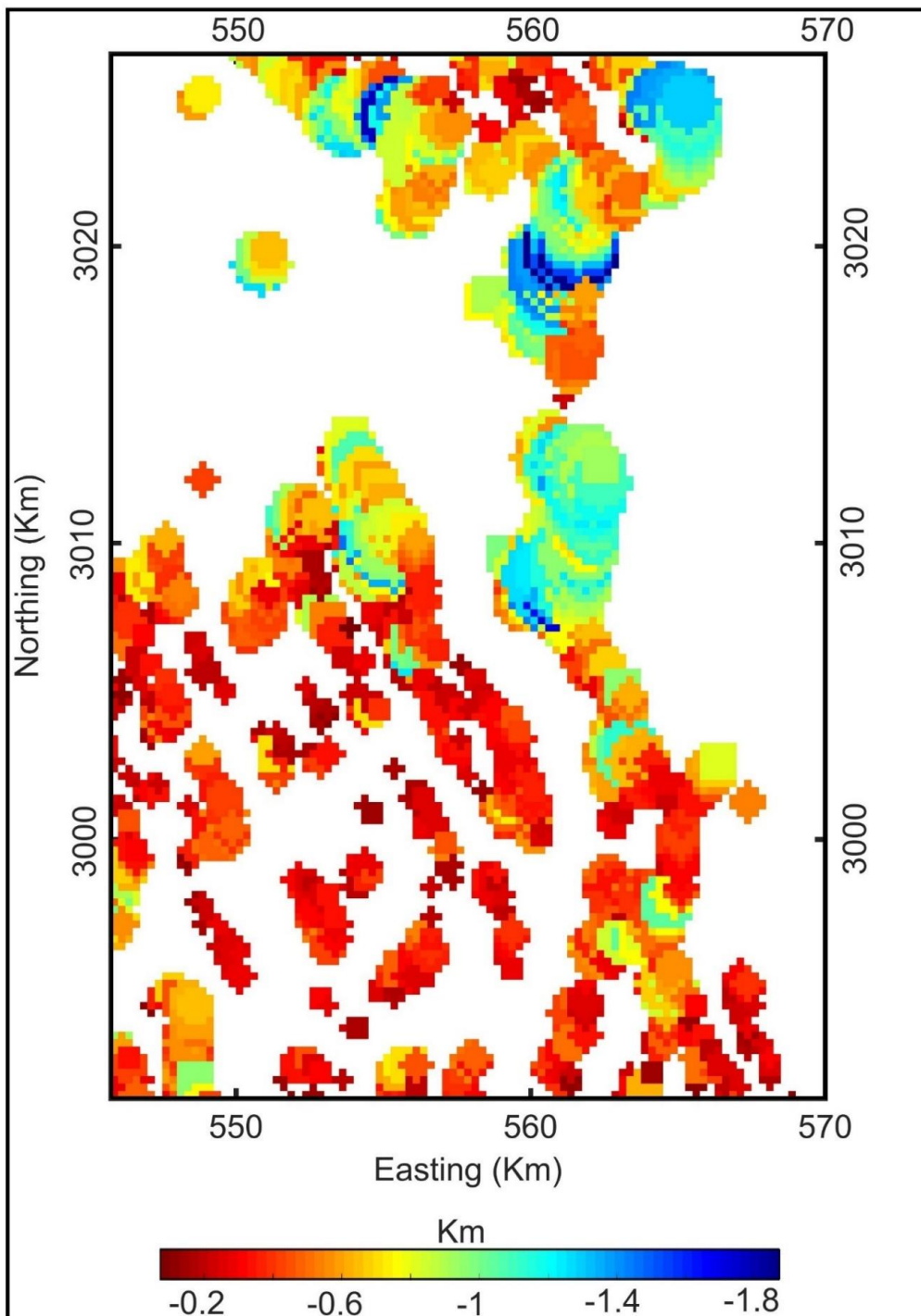


Fig. 6. Tilt depth contour map.

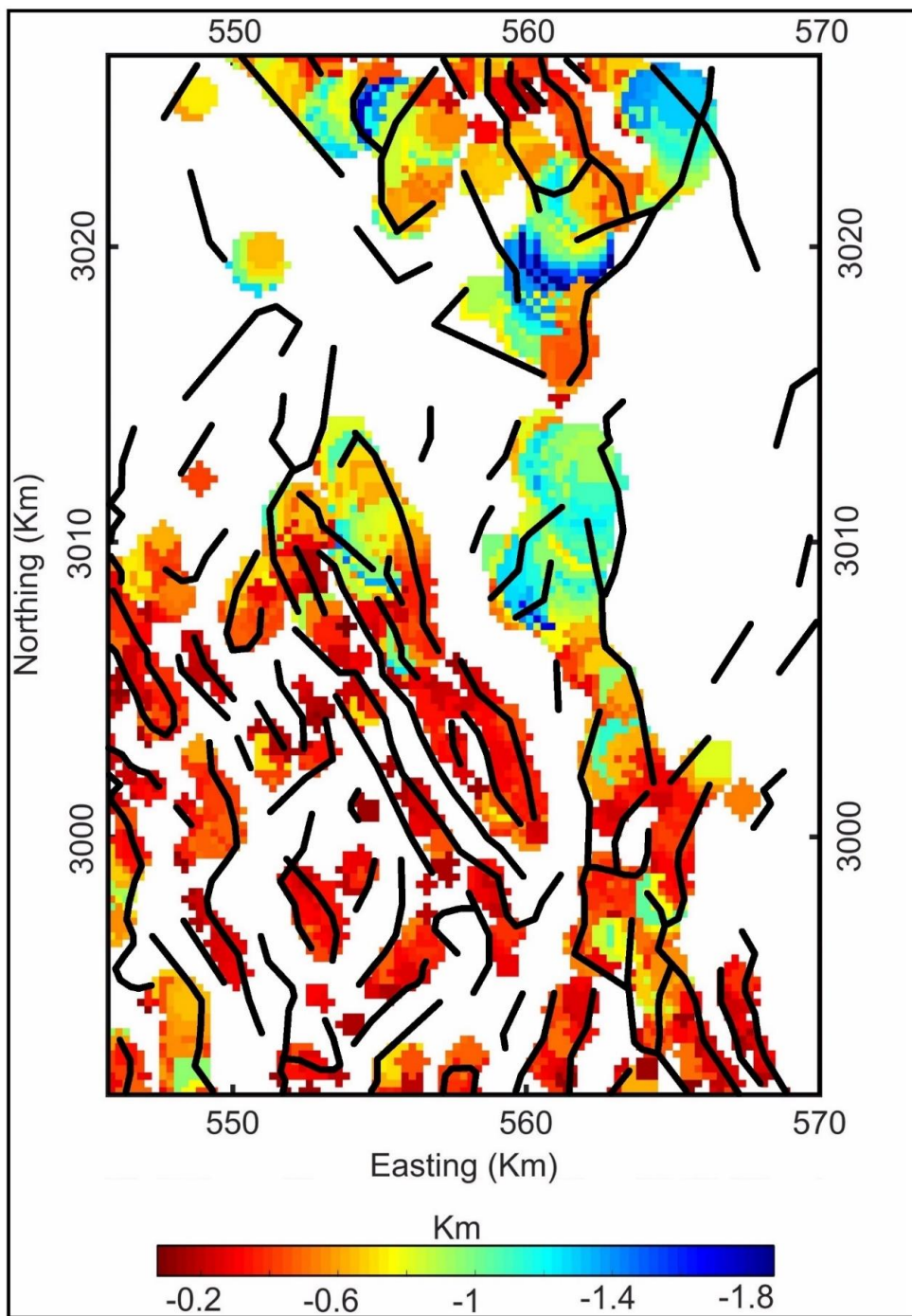


Fig. 7. Lineaments extracted from the FSED map and tilt depth contour map.